Mol Genet Genomics (2010) 284:273–287
DOI 10.1007/s00438-010-0565-0

ORIGINAL PAPER

Antler development and coupled osteoporosis in the skeleton of red deer *Cervus elaphus*: expression dynamics for regulatory and effector genes

Viktor Stéger · Andrea Molnár · Adrienn Borsy · István Gyurján · Zoltán Szabolcsi · Gábor Dancs · János Molnár · Péter Papp · János Nagy · László Puskás · Endre Barta · Zoltán Zomborszky · Péter Horn · János Podani · Szabolcs Semsey · Péter Lakatos · László Orosz

Received: 4 June 2010 / Accepted: 20 July 2010 / Published online: 10 August 2010
© Springer-Verlag 2010

Abstract Antlers of deer display the fastest and most robust bone development in the animal kingdom. Deposition of the minerals in the cartilage preceding ossification is a specific feature of the developing antler. We have cloned 28 genes which are upregulated in the cartilaginous section (called mineralized cartilage) of the developing ("velvet") antler of red deer stags, compared to their levels in the fetal cartilage. Fifteen of these genes were further characterized by their expression pattern along the tissue zones (i.e., antler mesenchyme, precartilage, cartilage, bone), and by in situ hybridization of the gene activities at the cellular level. Expression dynamics of genes *col1A1, col1A2, col3A1, ibsp, mgp, sparc*, *runx2,* and *osteocalcin* were monitored and compared in the ossified part of the velvet antler and in the skeleton (in ribs and vertebrae). Expression levels of these genes in the ossified part of the velvet antler exceeded the skeletal levels 10–30-fold or more. Gene expression and comparative sequence analyses of cDNAs and the cognate 5′ *cis*-regulatory regions in deer, cattle, and human suggested that the genes *runx2* and *osx* have a master regulatory role. GC–MS metabolite analyses of glucose,

Communicated by S. Hohmann.

Electronic supplementary material The online version of this article (doi:10.1007/s00438-010-0565-0) contains supplementary material, which is available to authorized users.

V. Stéger · A. Molnár · A. Borsy · I. Gyurján · Z. Szabolcsi · S. Semsey · L. Orosz (✉)
Department of Genetics, Eötvös Loránd University, Pázmány Péter s. 1/c, 1117 Budapest, Hungary
e-mail: orosz@abc.hu

V. Stéger · A. Molnár · A. Borsy · I. Gyurján · Z. Szabolcsi · G. Dancs · P. Papp · E. Barta · L. Orosz
Institute of Genetics, Agricultural Biotechnology Center, Szent-Györgyi Albert u. 4, 2100 Gödöllő, Hungary

J. Nagy · Z. Zomborszky · P. Horn
Department of Fish and Pet Animal Breeding, Faculty of Animal Science, University of Kaposvár, Guba Sándor u. 40, 7400 Kaposvár, Hungary

L. Puskás
Laboratory of Functional Genomics, Biological Research Center, Hungarian Academy of Sciences, P.O. Box 521, 6701 Szeged, Hungary

P. Lakatos
1st Department of Internal Medicine, Semmelweis University, Korányi Sándor u. 2/a, 1083 Budapest, Hungary

J. Molnár
BIOMI Ltd., Szent-Györgyi Albert u. 4, 2100 Gödöllő, Hungary

J. Podani
Department of Plant Taxonomy and Ecology, Eötvös Loránd University, Pázmány Péter s. 1/c, 1117 Budapest, Hungary

E. Barta
Apoptosis and Genomics Research Group of the Hungarian Academy of Sciences, University of Debrecen, Egyetem tér 1, 4010 Debrecen, Hungary

A. Molnár
Institute of Experimental Medicine of the Hungarian Academy of Sciences, Szigony u. 43, 1083 Budapest, Hungary

A. Borsy
Institute of Biochemistry, Biological Research Center of the Hungarian Academy of Sciences, Temesvári krt. 62, 6701 Szeged, Hungary

phosphate, ethanolamine-phosphate, and hydroxyproline utilizations confirmed the high activity of mineralization genes in governing the flow of the minerals from the skeleton to the antler bone. Gene expression patterns and quantitative metabolite data for the robust bone development in the antler are discussed in an integrated manner. We also discuss the potential implication of our findings on the deer genes in human osteoporosis research.

Keywords Antler cycle · Antler microarray · Physiological osteoporosis · Mineralization genes · Red deer · Osteocalcin · Runx2 · Osx

Abbreviations

AGC	Antler growth center
BMD	Bone mineral density
BMP	Bone morphogenetic protein
BGLAP	Human ortholog of *osteocalcin*
CGRP	Calcitonin gene-related peptide
Col1A1	Collagen alpha-1(I) chain
CVA	Canonical variates analysis/discriminant analysis
ECM	Extracellular matrix
FGF2	Fibroblast growth factor 2
GC–MS	Gas chromatography–mass spectrometry
Oc	Osteocalcin, human ortholog BGLAP
Osx	Osterix
PBS	Phosphate-buffered saline
PCA	Principal components analysis
PNP	Non-osteoporotic patients
PP	Patients affected with age-related osteoporosis
PTH	Parathyroid hormone
PTHrP	Parathyroid hormone-related protein
Runx2	Runt-related transcription factor 2
TGF	Transforming growth factor
TGFβ	Transforming growth factor beta

Introduction

An extremely intensive form of skeletal osteoporosis, termed cyclic physiological osteoporosis developed in deer stag. It is associated with antlerogenesis where the most robust bone development of the animal kingdom takes place. The pair of these two contrasting processes, antler ossification and skeletal osteoporosis, contributes to the reproductive success of the individual. Antlers are male secondary sexual characteristics and used for display and in combat. They are bony appendages of the deer's head, which are cast and re-grown each year. The development of antlers is a modified endochondral ossification process (Rucklidge et al. 1997). After casting, antler re-growth is initiated at the distal rim of the pedicle, where cells de-differentiate into embryonic stem cells (Li and Suttie 2001). These mesenchymal cells sequentially proliferate and differentiate into chondroblasts and chondrocytes associated with the formation of cartilage. The transition from undifferentiated cells to chondrocytes is gradual. The longitudinal growth proceeds proximal to distal from the pedicle, while the differentiation points to the opposite direction, from the tip to the base. The matrix of the antler cartilage is biochemically similar to that of other hyaline cartilages; however, it is well vascularized, and ossified bony trabeculae are formed on the cartilage scaffold by mineral deposition (Banks and Newbray 1981a, b). Calcification and ossification gradually occlude the blood supply to the antlers. When growth stops, transformation to bone is completed (Fig. 1) (Banks and Newbrey 1983), the velvet skin is shed; the antler is polished and ready for the rutting season (for a comprehensive overview see a recent review by (Price and Allen 2004). Since the growth rate of the antler may reach over 100 g per day between May and July, enormous bone mass (generally 7–9 kg, occasionally 13–15 kg, as reported from the Danube-Drava-Gemenc-Bilje National Park in Hungary and Croatia) develops within 100–120 days (the skeletal mass is estimated to be 15% of the live weight of the stags, about 30 kg in our case). The demand for mineral precursors surmounts the dietary intake by browsing. As a consequence, the gap is filled by mobilizing minerals from the skeleton, thus causing a temporary bone loss termed cyclic physiological osteoporosis (Banks et al. 1968a, b; Chapman et al. 1975). This phenomenon resembles human (pathological) osteoporosis both in its visual appearance and in its genetic background (Borsy et al. 2009). Before the rutting season, during the fitness recovery period in July and August, the process is reversed and bone mineral density (BMD) is restored. Mineral resorption is the highest, reaching 23%, in the rib cage and after reaching maximum antler growth it falls to less than 3% (Chapman et al. 1975).

Previously we identified a set of genes which are differentially expressed during the rapid but controlled tissue proliferation (Korpos et al. 2005; Molnar et al. 2007; Gyurján et al. 2007; Villányi et al. 2008) and another set, which is involved in the skeletal physiological osteoporosis (Borsy et al. 2009). In this work, we developed an antler-specific cDNA microarray in order to compare gene expression levels in the tissues of the mineralizing velvet antler and the skeleton (ribs and vertebra) of deer stags. Our results demonstrate the robust expression of genes *col1A1, col1A2, col3A1, ibsp, mgp, sparc*, and *osteocalcin* in the ossified part of the velvet antler. Results also suggest that overexpression of the transcription factor genes *runx2* and *osx* (Nakashima et al. 2002; Komori 2010) are key elements in the upregulation of the above genes. We attempt to integrate the gene expression data and GC–MS metabolite analyses to explain the bone mineral "traffic" between

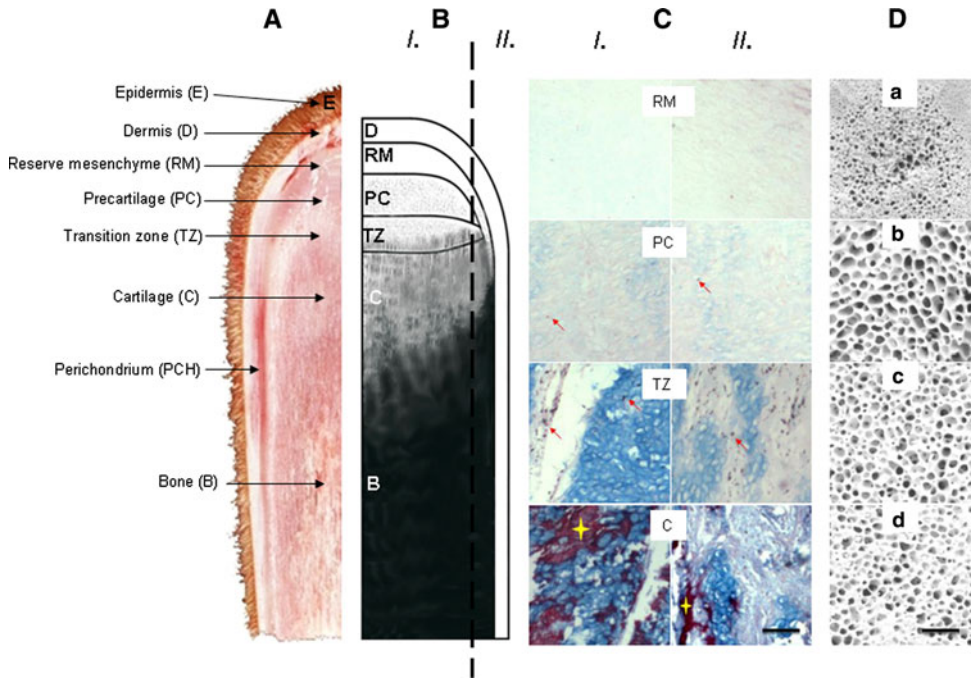

Fig. 1 Histology of the developing antler. **a** Parasagittal section of the velvet antler tip. **b** Schematic drawing of the progress of mineral depositions (modified from Banks and Newbrey 1981); *density of black dots* corresponds to mineral density and pattern. Note the conical shape of the mineralized cartilage-bone border. **c** Alcian blue/alizarin red staining: *blue* progression of glycosaminoglycan levels, *red* calcium in the extracellular matrix. I and II in **b** and **c**, inner and outer tissue regions, respectively. *Bar* 0.25 mm. **d** Structure of bone samples: *a* ossified part of the velvet antler of Stag 1(in antler development and skeletal osteoporosis status), *b* vertebral body of Stag 1(in antler development and skeletal osteoporosis status), *c* vertebral body of Stag 3 (in the velvet shedding, skeletal regenerating status), *d* vertebral body of Stag 2 (in the period of late autumn dwell status when mineral mobilization and deposition are dynamically equilibrated—BMD steady state). *Bar* 3 mm. (For more information see "Materials and methods", ESM Figure S1 and Borsy et al. 2009)

the antler and the skeleton. We also draw attention to the potential use of deer genes in human osteoporosis research.

Materials and methods

Collection of tissue samples of a red deer stag

Velvet antler and skeletal bone samples were collected from a red deer stag shot at the Deer Farm of Pannon Equestrian Academy, Bőszénfa, Hungary. Tissue collections were performed according to the Hungarian Animal Rights Law (243/1998, XII. 31). The time of tissue collection was during the period of active mineralization of the antler, at the beginning of June, when skeletal osteoporosis takes place. Deer fetuses were collected from hinds shot for selection purposes in late December and early January. Samples were stored under liquid nitrogen within 30 min after shooting.

Velvet antler samples

The velvet antler, grown for 90 days before the stag was shot at the beginning of June, was removed (kept in ice) and dissected. Positions of soft tissue layers (reserve mesenchyme, precartilage, and cartilage) of the growing antlers were determined as described by (Li et al. 2002). Since the potential for cross-region contamination was believed to be considerable, precautions were taken: the transition zones (easily recognizable by naked eyes) were sliced out with some "pure" tissues from both the upper and down layers. These slices (~0.3–0.5 cm thick) were discarded. The slices (~0.5 cm thick) containing the "pure" tissues were cut in two parts, one of them was fixed, sectioned, stained and used as a histological control, the other part was stored in liquid nitrogen and kept for mRNA preparations (Molnar et al. 2007; Gyurján et al. 2007). Bone samples of the velvet antler were taken from the section between the developing trez and brow tines (trez tine: royal or middle tine, the third tine of the antler from the head of the deer; brow tine: the first tine of the antler from the head). It is worth mentioning that the stag (Stag 1) was an 8-year-old capital individual (capital individual: stag of exceptionally strong antlers, the trophy would score at least 170 CIC points, i.e., at least a bronze medalist), his last year cast antlers weighed more than 8 kg.

Skeletal bone samples

Ribs and vertebras removed from the killed Stag 1 were extensively washed in PBS for eliminating blood and marrow contamination and then immediately frozen in liquid nitrogen. Both the inner part of the ribs and the body of the vertebras displayed an extremely porotic and fragile bone structure in the stag having velvet antlers (see Fig. 1d). In stags shot in the velvet shedding phase (late July, Stag 3's hard antlers weighed 8.1 kg) and in the late autumn dwell (end of November, Stag 2'shard antlers weighed 7 kg) the bones were no more porotic, their BMD and bone structure was restored (see more details in Borsy et al. 2009, and in Supplementary Material attached, ESM Fig. S1).

Fetal cartilage samples

Fetal cartilages were collected with the help of the professional hunter employee of the farm, where the balance between males and females should be maintained, and sorting out is unavoidable. The ~4-month-old fetuses were dissected, and the epiphyseal growth plates of long bone precursors were collected (Molnar et al. 2007; Gyurján et al. 2007).

Human bone tissue samples and real-time RT-PCR

Gene expression profiles in bone samples were determined in seven postmenopausal, unrelated, consecutive, Hungarian, Caucasian women suffering from age-related osteoporosis (PP group). The control group included ten bone tissue samples from postmenopausal non-osteoporotic, healthy women (PNP group). Sampling and measuring gene expressions were performed as described in Balla et al. (2007) and Borsy et al. (2009).

Total RNA purification from bone samples of red deer stags

Deer bone samples were cryoground under liquid nitrogen and extracted with acidic phenol–chloroform. Total RNAs were precipitated from the aqueous phase with LiCl and dissolved in 50 µl RNase-free water following DNase treatment.

Quality control of RNA samples

Quality of the isolated RNA was tested by capillary gel electrophoresis using 2100 Bioanalyzer and RNA 6000 Pico Kit (Agilent Inc, Santa Clara, US).

Construction and screening of lambda cDNA libraries

cDNA libraries were constructed from the three antler tissue zones mentioned earlier in the "Collection of tissue samples" using the SMART cDNA Library Construction Kit (Clontech), according to the manufacturer's protocol. Briefly, 1 µg mRNA samples were reverse transcribed with CDSIII oligo (dT) primer and SMART IV oligo provided by the kit using SuperScript II RNaseH-minus reverse transcriptase (Invitrogen). Each reaction volume was 20 µl. Long distance PCRs were performed in 50 µl reaction volume using 1 µl from the first-strand cDNA reaction, 1 µl dNTP mix (10 mM each), 5 µl 10× BD Advantage2 PCR Buffer, 10 M primers, 1 µl 50 Advantage Polymerase Mix and 1 µl (5 U) KlenTaq LA DNA Polymerase Mix (Sigma). Cycling parameters were 94°C for 5 min (initial denaturation), 25 cycles at 94°C for 1 min and 68°C for 7 min. Five microliter double-stranded cDNA samples were checked by electrophoresis in 1% agarose gel and after phenol–chloroform purification and ethanol precipitation 3 µg digested with *SWI*. Size fractionation was done by using SizeSep 400 (Pharmacia) chromatography column and the resulting product was ligated into the *SWI* digested, dephosphorylated λ TriplEx2 vector. For in vitro packaging 1 µl ligation reactions were used and $1–2 \times 10^6$ recombinant pfu were further propagated in XL1 Blue strain to get amplified libraries with $10^9–10^{10}$ pfu/ml. Library screening was performed according to the standard protocol (Sambrook et al. 1989). Approximately $2–3 \times 10^4$ phages were plated on Petri dishes of 180 mm diameter and plaques were lifted to GeneScreen hybridization transfer membrane (Perkin Elmer Life Sciences).

"Antler" microarrays, probe preparation, and hybridization

The SMART cDNA Library (see above) were converted to plasmid clones (according to the SMART™ protocol) in the *Escherichia coli* BM25.8 strain. After colony PCR amplification 3200 cDNAs were selected randomly for microarray construction. cDNA inserts from the lambda cDNA libraries generated from fetal growth plate, from velvet antler tissues mesenchyme, precartilage, cartilage were amplified by PCR with plasmid-specific primers and purified with MultiScreen-PCR plate (Millipore, Billerica, MA, USA), resuspended in 50% dimethyl sulfoxide, and arrayed on FMB cDNA slides (Full Moon BioSystems, Sunnyvale, CA, USA) using a MicroGrid Total Array System (BioRobotics, Cambridge, UK) spotter with 16 pins in a 4 × 4 format. Amplified cDNAs were printed in duplicate. The diameter of each spot was ~200 µm. Prior to hybridization the slides were blocked in 1xSSC, 0.2% SDS, 1% bovine serum albumin for 30 min at 42°C, washed in water and dried. For probe preparation, 5 µg of total RNA was reverse transcribed using poly-dT primed Genisphere Expression Array 350 Detection Kit system (Genisphere, Hatfield, PA, USA) according the to manufacturer's instruction. cDNA with capture sequence was hybridized onto cDNA

microarray. Both the first step cDNA hybridization and the second step capture reagent hybridization were carried out in a Ventana hybridization station (Ventana Discovery, Tucson, AZ, USA) by using the "antibody" protocol. First hybridization was performed at 42°C for 6 h in "FGL2" hybridization buffer (10× Denhardt solution, 0.25 M sodium phosphate buffer pH 7.0, 1 mM EDTA, 1× SSC, 0.5% SDS), and then 2.5 µl of Cy5 capture reagents was added to the slides in 200 µl "Chiphyb" hybridization buffer (Ventana) and incubated at 42°C for 2 h. After hybridization, the slides were washed in 0.2× SSC twice at RT for 10 min and then dried and scanned. Scanning and data analysis were done as described earlier (Puskás et al. 2002; Gyurján et al. 2007).

Northern blot analysis

Tissue samples (approximately 300 mg) were homogenized in guanidinium-thiocyanate and extracted with acidic phenol–chloroform. RNAs were precipitated from the aqueous phase with 3 M LiCl and dissolved in 30 µl RNase-free water. RNA concentrations were determined by measuring the absorbance at 260 nm. Five microgram aliquots of total RNA were separated by electrophoresis in 1.2% formaldehyde agarose gels. RNA was blotted to Hybond N+ filter (Amersham) according to the manufacturer's protocol. Fifty nanograms of cDNA fragments were labeled with [α^{32}P] dATP using random hexamers and *E. coli* DNA Polymerase I Large (Klenow) Fragment. The hybridization was performed at 65°C in the Perfecthyb TM Plus buffer (Sigma). After hybridization, the filters were washed at the same temperature according to the manufacturer's protocol. The signals obtained were evaluated using a PhosphorImager™ and quantified with STORMTM imaging system (Molecular Dynamics) and by the GeneTools program from Syngene.

Affymetrix microarray analysis

Expressions of deer genes (antler bone vs. vertebrae) were analyzed on *Bos taurus* 24K cDNA microarrays (GeneChip® Bovine Genome Array Affymetrix). Total RNA extraction, labeling, hybridization, quantity and quality controls were done as described in details in (Galamb et al. 2010).

In situ hybridization

The velvet antler tip was dissected and fixed in 4% (w/v) paraformaldehyde in PBS. Blocks were embedded in low-melting-point paraffin (Paraplast, Sigma) and sectioned longitudinally. Sections were mounted on slides coated with (3-aminopropyl) triethoxy-silane. Sections were then dewaxed, rehydrated and digested with Proteinase K and acetic anhydride, and hybridized overnight. RNA probes were labeled with digoxigenin-UTP (Roche) by in vitro transcription of the T7 RNA polymerase (cDNA template was cloned in TriplEx2 vector in the antisense orientation behind T7 promoter). The hybridization temperatures chosen were specific for the probes. After hybridization, the sections were washed in 2× SSC, 50% formamide, 2× SSC, for 30 min each at the hybridization temperature. Then the sections were treated with RNase H for 30 min at 37°C and then washed twice in 0.2× SSC. Digoxigenin was detected using sheep anti-digoxigenin alkaline phosphatase Fab fragments (Roche), followed by an alkaline phosphatase reaction using nitro-tetrazolium blue chloride and 5-bromo-4-chloro-3-indolyl phosphate as substrate. Sections were mounted using Kaiser's glycerin gelatine.

Extraction and analysis of metabolites by GC–MS

For GC–MS analysis, polar metabolite fractions were extracted from 60 mg of each frozen material. Sample preparation, derivatization, and metabolite analysis were carried out by the method of (Nikiforova et al. 2005). Ribitol was added for internal standardization. Samples were injected in splitless mode (1 µl/sample) and analyzed in a quadrupole-type GC–MS system (Finnigan Trace/DSQ, Thermo Electron Corp.). The chromatograms and mass spectra were evaluated by using the XCALIBUR software (Thermo Electron Corp.) and the NIST 2.0 library.

Bioinformatics

All sequence manipulations were done in UNIX environment using standard BASH and PERL scripts. Promoter sequences were obtained from ENSEMBL and DOOP databases (Barta et al. 2005). Motif searching and other sequence analysis tasks were carried out using the programs from the EMBOSS package.

Statistical analyses

The differential expression of 15 human orthologs of identified deer genes (*col1A1, col1A2, col2A1, col3A1, col10A1, mgp, sparc, eno1, fabp3, serf2, anxa1, tmsb4x, tmsb10, oc/BGLAP,* and *runx2*) in osteoporotic versus non-osteoporotic patients were detected with relative quantitative real-time RT-PCR analysis as described in Borsy et al. (2009). Gene expression data were evaluated by multivariate statistical analyses according to Borsy et al. (2009), principal components analysis (PCA) and canonical variates analysis (CVA or discriminant analysis) using the SYNTAX 2000 program package (Podani 2001).

Results

Identification of genes upregulated in the mineralized cartilage of the velvet antler

Our major goal was to identify genes, which are involved in the extremely rapid and robust mineralization of the ossified part of the developing velvet antler. A well-established observation provided a solution, namely, that the chondrogenic tissues of the velvet antler are mineralizing in contrast to the fetal cartilage; nonetheless, the matrix of the two is biochemically similar regarding the major components (Price et al. 2005). Therefore, comparison of the antler precartilage and cartilage versus fetal cartilage can pinpoint a subset of differentially expressed genes, which are important for the robust antlerogenic mineralization and ossification.

In order to make identification and isolation of "antler specific" genes efficient, we made an antler cDNA microarray. In this "antler" microarray (see "Materials and methods") 3200 randomly chosen cDNAs were arrayed, representing the gene expression in three successive tissues of the antler tip: mesenchyme, (mineralized) precartilage, and cartilage.

The mRNAs of the cognate samples (i.e., precartilage and cartilage) of the velvet antler were probed against the fetal cartilage mRNA pool (on the "antler" microarray). The histological control showed that the "purity" of the (antler) precartilaginous tissue samples was more than 90% for (pre)chondroblasts, but a small percentage of chondrocytes was generally also detected; samples from the antler cartilage consisted of only chondrocytes (i.e., no (pre)chondroblasts or osteoblasts were observed). In the matrices of the precartilage and cartilage, mineral depositions were detected by alizarin red staining (Fig. 1c). The fetal growth plates consisted of ~90% chondrocytes and ~10% osteoblasts. No (pre)chondroblasts and mineralization were recorded in this cartilage (Korpos et al. 2005; Molnar et al. 2007). These histological patterns (i.e., for cell types) supported the above-mentioned rationale that by subtracting the expression levels of the fetal growth plate from that of the antler cartilaginous samples we could detect genes, which express in the early stages (i.e., in the antler (pre)chondroblasts and chondrocytes), of the robust ossification.

We sequenced 66 candidate cDNA inserts, which showed elevated expression in the antler cartilage tissues over the fetal growth plate. The expression-fold differences scattered between 1.7 and 5.3 (Table 1). These 66 cDNAs corresponded to 28 genes, belonging to various functional groups: 8 genes code for proteins known to be associated with skeletal development (i.e., ossification, phosphate transport, calcium ion binding, extracellular matrix, Table 1A), and 10 genes which underline the elevated metabolic demands of the rapid growth (energy transport, ribosomal proteins, Table 1D); 4 genes out of 28 were so far unannotated putative genes (Table 1C), the remaining 6 genes were well defined, but with unknown role in cartilage or bone metabolism (Table 1B). We chose the 14 genes listed in Table 1A and B for further analysis.

Bioinformatical analysis of the regulatory regions of the selected genes

The cloned deer cDNA sequences were very similar to the corresponding *Bos taurus* (*Bos, cattle*) sequences (95–98% homology). We were also interested in the similarities of the 5′ regulatory regions of the selected deer genes and their *Bos taurus* orthologs. First we compared the regulatory regions of the *col1A1* orthologs because this gene is one of the most exhaustively investigated and utilized genes in bone research and in human clinical practice. We PCR amplified 1kbp of the 5′ upstream sequence of the gene *col1A1* together with the first exon (one primer was designed for the deer cDNA, and the other for the *Bos* 5′ upstream sequence), determined the sequence of the PCR product, and then compared it with the corresponding human and *Bos* regions. As shown in Fig. 4, the homology between deer and human, and *Bos* and human was 80 and 82%, respectively, while between deer and *Bos* it was as high as 93%. This value was close to what was observed for the cDNAs (97%), indicating the evolutionary closeness of the two species. The sequences contained many binding sites for the known bone master regulators Runx2 (also named Cbfa1) and Osx: 13, 14, 17 (for Runx2), 18, 15, 17 (for Osx) for human, *Bos,* and deer, respectively, with colinearity seen in their arrays (Fig. 4; Table 2, ESM Figs. S4 and S5).

The large number of the Runx2 and Osx binding sites in the deer *col1A1* promoter region prompted us to analyze the available sequences of the 5′ control regions of the bovine and human orthologs of the upregulated antler genes (i.e., those 14 of Table 1A, B). The *runx2 and osx* genes were also included in the analysis, together with one of the primary targets of Runx2, the osteocalcin/*BGLAP* (*oc*) gene. The *oc* gene encodes a hormone-like protein factor (Oc, Lee et al. 2007), which is involved in bone regeneration/development. The osteocalcin protein level is a standard reference marker for BMD (Siebel et al. 2002). We found that all the genes contained a large number of binding sites for the transcription factors, Runx2 and Osx (Table 3 and ESM Figs. S4 and S5).

Expression patterns of the selected genes in the velvet antler

The expression patterns of the above 17 Runx2 and Osx regulated genes were further studied by Northern hybridization.

Table 1 Genes upregulated (1.7- to 5.3-fold expression differences) in the cartilaginous tissues of the developing antler versus growth plate cartilage using "antler microarray"

Gene name	Times	Accession number	Biological process	Molecular function
A: Genes previously associated with skeletal development				
Collagen, type I, alpha 1 (*col1A1*)	13	EF619481	Skeletal development, ossification	The major extracellular matrix of bone
Collagen, type I, alpha 2 (*col1A2*)	4	FN868903	Skeletal development,	Structural constituent of bone
Collagen, type II, alpha 1 (*col2A1*)	8	FN868904	Skeletal development,	Extracellular matrix
Collagen, type III, alpha 1 (*col3A1*)	2	FN868905	Phosphate transport	Extracellular matrix structural constituent
Collagen, type X, alpha 1 (*col10A1*)	1	FN868906	Skeletal development	Calcium ion binding
Matrix Gla protein (*mgp*)	2	FN868907	Bone mineralization, cartilage, ossification	Extracellular matrix structural constituent, calcium ion binding
Secreted protein, acidic, cysteine-rich (osteonectin) (*sparc*)	2	FN868902	Ossification	Calcium ion binding, collagen binding
Integrin-binding sialoprotein (*ibsp*)	2	FN868908	Ossification cell adhesion	Protein binding
B: Not associated with skeletal development				
Enolase 1, (alpha) (*eno1*)	1	EF619484	Metabolic process protein ubiquitination	Protein binding, metal ion binding
Fatty acid binding protein 3 (*fabp3*)	1	FN868909	Transport	Transporter activity, fatty acid binding
Small EDRK-rich factor 2 (*serf2*)	1	FN868910	Regulation of transcription,	DNA binding, protein binding
Annexin A1 (*anx1*)	1	FN868921	Cell cycle	Phospholipase inhibitor
Thymosin beta 4, X chromosome (*tmsb4x*)	4	EF619493	Cytoskeleton organization	Actin binding
Thymosin beta 10 (*tmsb10*)	3	FN868911	Cytoskeleton organization	Actin binding
C: Putative genes				
Putative genes, clone p424	1	FN868912	Unknown	Unknown
Putative genes, clone p425	2	FN868913	Unknown	Unknown
Putative genes, clone p426	1	FN868914	Unknown	Unknown
Putative genes, clone p427	2	FN868915	Unknown	Unknown
D: Genes for high metabolic demands				
Chaperonin containing TCP1, subunit 8 (theta) (*CCT8*)	1	FN868916	Protein folding	Nucleotide binding, protein binding, unfolded protein binding
Mitochondrially encoded cytochrome *c* oxidase II	10	FN868917	Energy, electron transport	Component of the respiratory chain
Cytochrome *c* oxidase subunit VIIc	1	FN868918	Energy, electron transport	Component of the respiratory chain
Mitochondrially encoded cytochrome *c* oxidase III	1	FN868919	Energy, electron transport	Component of the respiratory chain
Ribosomal protein S8	2	FN868920	Translation	Constituent of ribosome
Mitochondrial ribosomal protein S12	1	FN868922	Translation	Constituent of ribosome
Ribosomal protein L18a	1	FN868923	Translation	Constituent of ribosome
Ribosomal protein, large, P1 (*RPLP1*)	1	FN868924	Translational elongation	Constituent of ribosome
Mitochondrially encoded ATP synthase 6	1	FN868925	Energy, electron transport	Component of the respiratory chain
Ornithine aminotransferase	1	FN868926	Ornithine metabolic process	Ornithine-oxo-acid transaminase activity, protein binding

The expression patterns obtained are consistent with the results of microarray screenings (Fig. 2, ESM Table S1). All the investigated genes are expressed in the precartilage as well as in the cartilage zones. Three of these genes (*col3A1*, *fabp3, thymosin b10*) are predominantly expressed in the antler mesenchyme. The ossification marker genes, *col1A1, mgp, sparc,* and *ibsp* already showed high expression in the upstream developmental states i.e., in the antler mesenchyme, precartilage, and cartilage. The gene expression levels obtained in the antler tissues (including bone) and skeletal bones were quantified by measuring band intensities (Table 4, ESM Table S1). Results were normalized using the expression levels of the internal controls (18S and 28S rRNAs) and for the expression of the *gapdh*

Table 2 Number of DNA binding sites for transcription factors Runx2 and Osterix in the 5′ URS sequences (promoter) of the bos, human and deer orthologs genes

Genes	Runx2					Osx				
	Bt		Hs		Ce	Bt		Hs		Ce
	1K	5K	1K	5K	1K	1K	5K	1K	5K	1K
col1A1	14	59	13	58	17	15	86	18	98	17
col1A2	15	77	16	87		35	56	44	65	
col2A1	6	65	10	46		68	84	44	56	
col3A1	15	81	15	67		4	5	3	11	
col10A1	9	92	26	91		4	9	0	15	
mgp	17	72	16	68		5	8	1	8	
sparc	8	71	18	89		11	26	6	20	
ibsp	19	82	10	80		0	12	0	8	
eno1	8	70	6	73		29	40	31	55	
fabp3	11	70	7	74		25	58	24	46	
serf2	5	52	18	74		13	32	28	47	
anx1	13	73	27	68		1	2	2	6	
tmsb4x	9	12	20	62		22	28	39	56	
tmsb10	9	77	17	78		29	37	34	45	
oc	17	58	25	80		34	75	34	59	
runx2	34	88	40	85		3	7	1	5	
osx	9	61	20	86		30	60	28	77	

Sequences of 1 kbp (1K) and 5 kbp (5K) long were analyzed in silico (see software and database information in the "Materials and methods"). For gene TMSB4 sequences of 1,500 bp long were tested. Sp1 refers to the Osx binding site (*y*, Fig. 4) of diagnostical value for detecting human osteoporosis susceptibility (see more details in "Discussion")

Bt, *Bos taurus*; Hs, *Homo sapiens*; Ce, *Cervus elaphus*

Table 3 Homology (in %) of cDNA and 5′ URS (promoter) sequences of red deer, human and bovine orthologs

Genes	cDNA			Promoter[a]	
	Ce/Bt (%)	Ce/Hs (%)	Bt/Hs (%)	Bt/Hs (%)	
				1K	5K
col1A1	97	91	93	82	74
col1A2	98	91	90	94	74
col2A1	97	93	92	81	72
col3A1	97	91	88	82	80
col10A1	96	78	85	77	77
mgp	96	78	79	71	69
sparc	95	81	86	77	75
ibsp	95	83	80	77	77
eno1	92	79	86	86	73
fabp3	96	85	84	71	71
serf2	96	97	89	–	–
anx1	98	88	88	70	69
tmsb4x	96	86	86	72	70
tmsb10	98	87	88	66	66
oc	94	85	84	67	69
runx2	99	95	95	87	75
osx	96	85	84	82	77

Homologies in %: Ce/Bt, *Cervus elaphus* versus *Bos taurus*; Ce/Hs, *Cervus elaphus* versus *Homo sapiens*; Bt/Hs, *Bos taurus* versus *Homo sapiens*. Data based on BLAST program

[a] The homology of promoter sequences Ce/Bt is 93% (see text)

housekeeping gene. The genes *col1A1, col1A2, col3A1, ibsp, mgp,* and *sparc* were 2- to 10-fold upregulated in the antler cartilages and highly upregulated in the ossified part of the velvet antler, far more (10- to 30-fold or sometimes more) than in the ribs and vertebras (Fig. 2; Table 4, ESM Table S1, ESM Fig. S2). The expression differences in the antler and skeletal bones were also analyzed and evaluated independently using Bovine 24K Affymetrix microarrays and the same tendencies were recorded (Table 4).

As shown in Fig. 2 and Table 4 the expression levels of the BMD maker gene *oc* and of the genes for DNA binding transcription factors *runx2* and *osx* kept up with the high expression of the 'antler genes'. They gave very strong expression signals in the ossified part of the velvet antler, unlike in the ribs and vertebrae where their level remained under the detection level of the assay. However, in the antler cartilage, strong *osx* and *runx2* expression was observed but as expected the bone-specific marker gene *oc* was not expressed.

Expressions of bone marker genes in the antler chondroblasts and chondrocytes: spatial confirmation by in situ hybridization

It is widely accepted that expressions of the genes *col1A1, ibsp, mgp,* and *sparc* are indicators of bone mineral metabolism (Siebel et al. 2002). However, in the developing antler, these genes show strong expression not only in the bone but also in the earlier developmental states, which precede the formation of antler bone: (a) *col1A1* and *sparc* in the mesenchyme, precartilage, and cartilage; (b) *ibsp* and *mgp* in the precartilage and cartilage. These observations called for further investigations in order to assign the expressions to specific cell types. Therefore, we performed in situ histological localization of *ibsp*, *mgp*, *sparc*, and *col3A1* gene expressions. This technique was successfully used before to localize *col1A1*, *col2A1*, and *col10A1* expression in the growing antler (Price et al. 1996). In Fig. 3 and ESM Fig. S3 we show that all the four ossification indicator genes, similar to the *col2A1*(Gyurján et al. 2007) chondroblast/chondrocyte reference marker gene, are expressed in chondroblasts and chondrocytes. Beyond this, the in situ

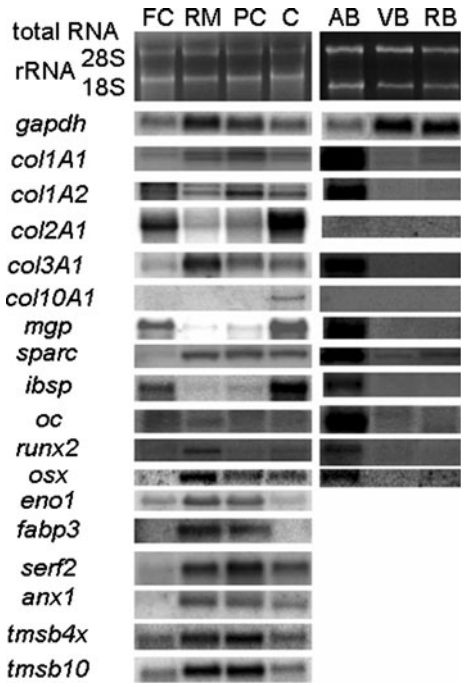

Fig. 2 Northern blot analyses of gene expressions. Antler tissues: *FC* fetal growth plate cartilage, *RM* antler reserve mesenchyme, *PC* antler precartilage, *C* antler cartilage, *AB* antler bone; Skeletal bones: *VB* vertebral bone, *RB* rib bone. Note the robust expressions in *AB* versus *VB* and *RB*, the cartilage specific expression of *col2A1* and *col10A1* and the over expression of *col1A1, col1A2, sparc, osx* and *runx2* in the antler tissues versus FC. (Further details are presented in Table 2, ESM Fig. S2, ESM Table S1)

Table 4 Expression-folds for genes in antler bone (AB) relative to skeletal bones (VB, RB) in Stag 1

Genes	28S rRNA control		gapdh control	Affymetrix array
	AB per VB	AB per RB	AB per VB	AB per VB
col1A1	>7.6	>6.9	>17.0	8.9
col1A2	>19.0	>11.0	>42.0	9.8
col2A1	i.m.	i.m.	i.m.	1.3
col3A1	>19.0	>15.0	>43.0	176.5
col10A1	i.m.	i.m.	i.m.	0.9
mgp	>10.0	>7.0	>28.0	33.1
sparc	>13.3	>5.8	>29.7	53.9
ibsp	>40.0	>30.0	>100	73.2
Oc	>7.0	>7.0	>15.0	10.3
runx2	>3.0	>4.0	>7.0	No data
osx	>28.0	>17.0	>63.0	No data
gapdh	0.4	0.3	1.0	0.6

Gene expressions were normalized to internal controls 28S rRNA and *gapdh* expressions. Fold changes were calculated from Northern blot analyses (see Fig. 2) using program SYNGENE, and from Bovine 24K Affymetrix microarray measurements. Since the thresholds for Northern detections of the expressivities in AB versus RB and VB were too far from each other only the lower approximates for the fold differences could have been calculated. At longer expositions clear Northern signals can be detected in AB and VB for *col1A1*, *col1A2*, *ibsp*, *sparc* (for *ibsp* see ESM Fig. S2)

Values for 18S rRNA normalization control were very close to those shown for 28S rRNA, data not shown

AB antler bone, *VB* vertebral bone, *RB* rib bone, *i.m.* incommensurable

expression hybridization of the *col1A1* and *sparc* genes was also detected in the mesenchymal cells. The gene expression pattern of *col3A1* was similar to that of *col1A1,* while *col10A1* expressed exclusively in the hypertrophic (antler) chondrocytes (ESM Fig. S3). It is worthwhile noting that the in situ hybridization of the gene expressions agreed perfectly with that expected after the Northern analyses (see Fig. 2).

Consumption of glucose and bone metabolites in the ossifying section of the antler: GC–MS analyses

The impact of the high overexpression of the antler genes on bone metabolism was measured in the antler and skeletal (vertebrae, rib) bone samples by GC–MS analyses (Table 5). Four parameters were monitored: (a) the level of hydroxyproline i.e., the conventional marker for collagen breakdown (hence for the loss of the organic material of the bone), (b) the free phosphate, (c) ethanolamine-phosphate levels (i.e., markers for the density of bone inorganic components), and (d) the glucose concentration ("energy consumption" marker for the activity for the Runx2–osteocalcin–insulin pathway (Siebel et al. 2002; Whyte 2002; Lee et al. 2007). As shown in Table 5, the GC–MS data agree with the gene expressions: the 6- to 7-fold lower levels for hydroxyproline and ethanolamine-phosphate, and the 40% lack in the free inorganic phosphate in the antler versus the levels in the vertebral body indicated the robust bone deposition in the antler at the expense of bone loss in the skeleton (similar tendencies were observed for the comparisons of antler bone vs. rib). The very high glucose level in the antler bone (fivefold over the vertebral body) was consistent with the high-energy consumption of the robust development of the antler bone, a consequence of the high anabolic activity along the Runx2–osteocalcin–insulin pathway.

Expression pattern of the orthologs of the deer genes in human osteoporotic and non-osteoporotic patients

Expression of the human orthologs of the 15 deer genes listed in Fig. 5 was previously determined in 7 osteoporotic and 10 non-osteoporotic patients (Borsy et al. 2009). Here we evaluated the expression patterns by PCA and CVA statistical analyses using the SYNTAX 2000 program package (Podani 2001). As shown in Fig. 5 CVA analysis discriminated unambiguously between osteoporotic and non-osteoporotic patients.

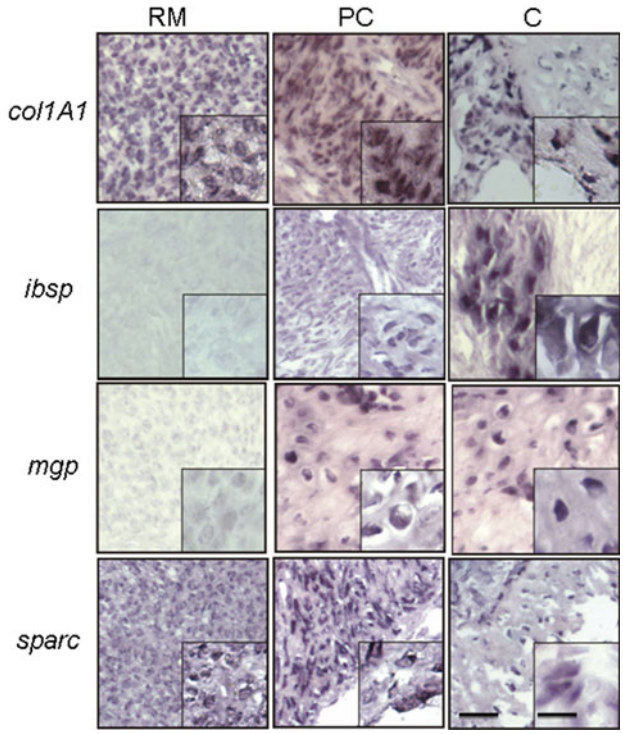

Fig. 3 Examples for in situ hybridization of gene expressions (mRNAs) in velvet antler tissues. Analyses of 8 µm thick longitudinal sections: (*RM*) from mesenchymal region, (*PC*) from precartilage, (*C*) from cartilage. *Bars* 0.25 and 0.1 mm in the *corners lower left* (the higher magnifications). Note the prominent expression of *col1A1* and *sparc* in all 3 tissues, *ibsp* and *mgp* in precartilage and cartilage (in situ hybridization for genes *col3A1* and *col10A1* are shown in ESM Fig. S3)

Table 5 Relative quantities of metabolites in antler bone (AB) and vertebrae bone (VB): GC–MS analyses

Metabolites	AB	VB
Glucose	26.77 ± 6.85	5.58 ± 0.25
Phosphate	15.82 ± 1.27	24.76 ± 2.69
Ethanolamine-phosphate	0.41 ± 0.17	2.62 ± 0.07
Hydroxyproline	0.32 ± 0.07	1.99 ± 0.22

Data refer to tissues samples of 1 mg. See more details in "Materials and methods"

As indicated by PCA ordination (Fig. 5 lower left) the expression patterns varied much less among the osteoporotic than in non-osteoporotic patients (note: the square white convex hull was much smaller than the black one).

Discussion

Regulation of bone metabolism in antlerogenesis

In this paper, we aimed to get an insight into the epigenetic regulation bone resorption and deposition in red deer stags during antlerogenesis. Changes in bone metabolism during this period are associated with two contrasting processes, the robust ossification in the developing velvet antler and the extremely intensive osteoporosis in the skeleton, which is termed cyclic physiological osteoporosis. We assumed that the identification of genes, which are related to the known histological characteristics of the antler cartilage, namely, its intensive pre-osteogenetic calcification, brings us closer to the answer. Therefore, we developed an "antler cDNA microarray" which allowed efficient, identification of deer genes upregulated in the cartilaginous zones of the developing velvet antler (28 genes in Table 1). The genes obtained belonged to different functional groups.

In this work we paid particular attention to those genes, which belong to a group which can be characterized as "bone reference marker or matrix genes". We found that these genes are highly expressed already in the (antler) chondrocytes and chondroblasts (Figs. 2, 3, ESM Figs. S2 and S3), 2- to 10-fold over the fetal growth plate cartilage level (ESM Table S1).

The expression patterns of these genes are in agreement with the contrast of the robust ossification of the antler versus the osteoporosis in the skeleton. Their expression level was much higher in the bony part of the velvet antler compared to the skeletal samples, ribs, and vertebras. We calculated 7- to 17-fold higher *col1A1* expression in the antler bone over the skeletal level when using various internal controls for computing (i.e., 18S rRNA, 28S rRNA, *gapdh*) and two independent approaches (Northern blot analysis combined with SYNGENE program, Affymetrix measurements). However, we note that the fold numbers must be interpreted with caution because the modified endrochondrial type bone development (i.e., antler) was compared here with the skeletal process. Even more robust expression differences were recorded for the other mineralization genes (Table 4). It would be interesting to see as to what extent these figures are adaptable for the female osteoporosis developing during gestation (for example, the severe sternal and iliac bone loss of the cow at calving has been known for long).

We assumed that the bone reference marker and matrix genes upregulated in the developing antler respond to the same transcriptional regulators, therefore by analyzing their promoter regions we can predict which transcription factors are involved in the regulation of mineralization. The high similarity of the deer and *Bos taurus* genes allowed PCR amplification of the promoter region of the deer *col1A1* gene. Sequence analysis of the amplified regulatory region unearthed a large number of the binding sites for the transcription factors Runx2 and Osx.

We suggest that the genes *runx2* and *osx* function in the antler as master regulators of the genes listed in Fig. 2. This view is supported by several lines of the experimental

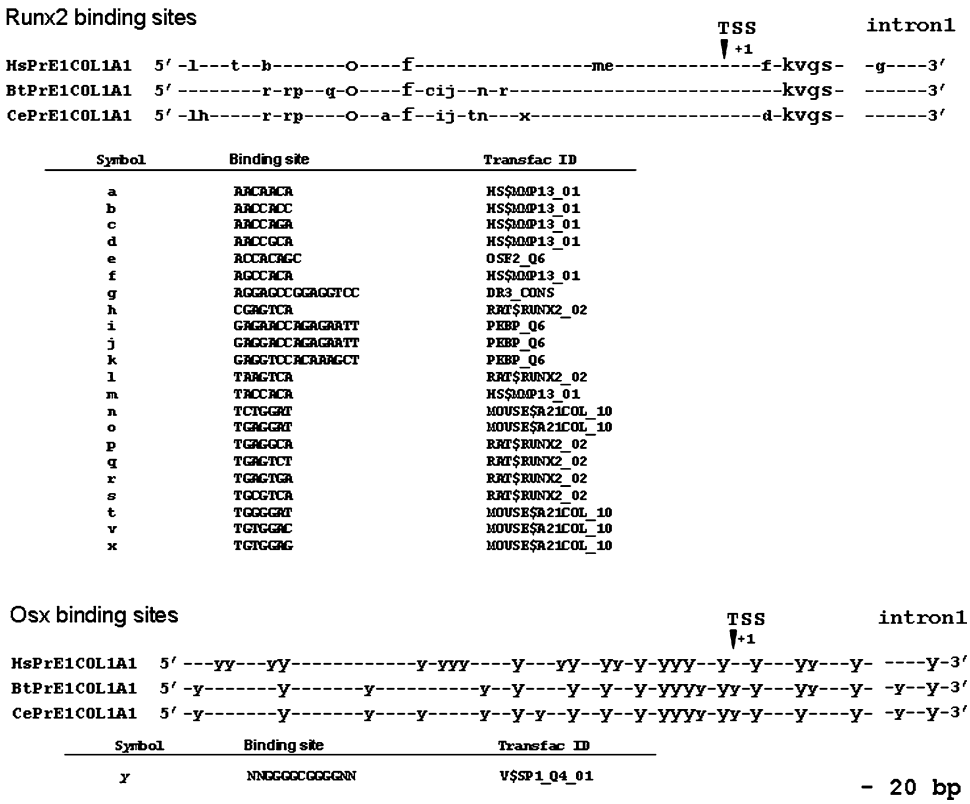

Fig. 4 Position of binding sites for transcription factors Runx2 and Osterix along the 1 kbp 5′ URS (promoter) sequence and first intron of *col1A1* gene orthologs (*Hs* human, *Bt* bovine, *Ce* red deer). Osterix binding site: y. TSS, starting point of mRNA synthesis. Note the co-linearity and commensurability for many positions (*in bold*) of the binding sites along the three orthologs (all details are presented at sequence levels in ESM Fig. S4, ESM Fig. S5). *One dash* corresponds to 20 bp

evidence. (a) As mentioned above, the first intron and the 5′ upstream sequence of the deer *col1A1* gene is rich in binding sites for Runx2 and Osx alike in *Bos* and human. Moreover, their array and often their spacing are conserved (co-linear/commensurable) in the three species (Fig. 4). (b) The 175 bp long sequence spanning over the Osx binding site *sp1* in the *col1A1* first intron is fully conserved in the ruminant and the man, except for two positions (Jin et al. 2009). This region contains the SNP site, which serves as a diagnostic marker for osteoporosis susceptibility in human, that is, the +1245G or T nucleotide position characterizing the *S* and *s* alleles of the *sp1* site is linked to bone density phenotypes (the *s/s* genotype is osteoporotic (Alvarez et al. 1999). (c) The *osteocalcin* gene, the primary target of *runx2* regulation in mammalian model systems (Stein et al. 2002), is also upregulated in the antler bone samples (Fig. 2). (d) All the orthologs of the upregulated antler genes (Fig. 4; Table 2) in *Bos* (and human) carry numerous Runx2 and Osx binding sites. Although the deer genomic sequences are not yet available, we assume that the promoters and cis-regulatory regions of the above deer genes show similar evolutionary conservation as we found in the case of *col1A1* (93%, Fig. 4).

Antler tip: runx2 pathway

Runx2 is essential for human osteoblastic differentiation and skeletal morphogenesis and acts as a scaffold for nucleic acids and regulatory factors involved in skeletal gene expression (Komori 2010; Kohen 2009). We detected the expression of *runx2* as well as its downstream target *osx* in the mesenchyme of the antler tip (Fig. 2, ESM Table S1), which indicated that these cells are already committed toward chondrogenesis and osteogenesis. From the upstream signals, which play determinant role in initiating the positive autoregulation of the *runx2* gene, strong expression of PTHrP (parathyroid hormone-related protein) has been demonstrated in the antler mesenchyme, precartilage, and prechondrium (Faucheux et al. 2002; Faucheux and Price 1999). A candidate for the upstream-most morphogene could be the calcitonin gene-related peptide (CGRP, see argumentation below).

In the vascularized antler cartilage, additional upregulating stimuli may also reach the cells by the blood stream, keeping the activity of the Runx2-Osx pathway high. Expression of the Runx2 activated genes encoding mineralization proteins (like *col1A1*) exhausts Ca and Mg from the blood. After the apoptosis of the chondrocytes, a prefabricated mineralized matrix is left behind, which is protected from proteolytic decay due to the mineral deposition. This space is then occupied by osteoblasts to form the ossified part of the developing antler. Our results are compatible with this scenario and are supported by both the gene expressions and the histological investigations: (a) large mineralized islands were identified in the antler cartilage (Fig. 1), (b) strong expressions of the mineralization genes

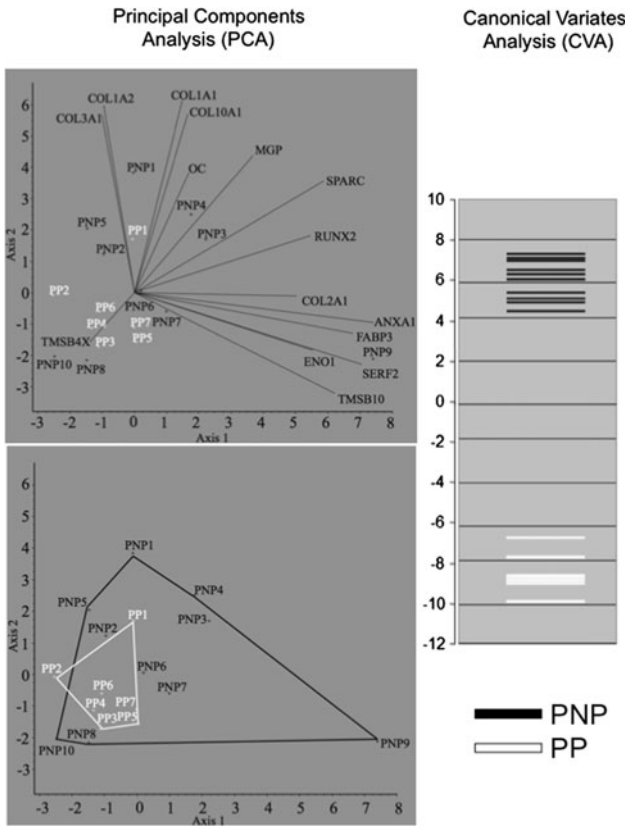

◀ **Fig. 5** Multivariate exploration of gene expression patterns in bone tissues of 7 osteoporotic (*white symbols*, labeled *PP*) and 10 non-osteoporotic (*black symbols*, labeled *PNP*) patients. The basis of the computations is a 15 × 17 data matrix **X** in which x_{ij} is the RQ (Relative quantity), i.e., the expression of gene *i* in patient *j*. Analyses are based on human orthologs of 15 deer genes (*col1A, col1A2 col2A1, col3A1, col10A1, mgp, sparc, eno1, fabp3, serf2, anx1, tmsb4x, tmsb10, oc/BGLAP, runx2*). *Left* Results of Principal Components Analysis (PCA) which summarizes multidimensional data structure in terms of a few important and uncorrelated dimensions called the components (Podani 2001). In this, excessive scale differences between variables (here genes) are eliminated by using standardized RQ values. *Upper left* PCA biplot showing simultaneous ordination of patients and genes. In the graphical biplot display for any two components, the observations (in this case, the patients) appear as points, the variables (here, the genes) are shown as vectors. The strength of influence of one gene on the others and the correlations are expressed by the vector lengths and the angle between them. This simultaneous representation allows for the evaluation of the grouping of patients and the assessment of the relative importance and correlation of genes influencing this configuration. Note the strong correlation between expressions of *fabp3* and *anx1, col1A1* and *col10A1*, *col1A2* and *col3A1*. This indicates that the activity changes of one of the gene of the pairs parallels with the activity changes of the other gene of the respective pair, both in the *PP* and *PNP* groups. Gene expressions are mostly downregulated in the post-menopausal osteoporotic patients as compared to the non-osteoporotic samples. The longer the vector, the higher is the ratio of expression alteration it shows. Angle between vectors is inversely proportional to the correlation between the expression of genes represented by the given vectors. *Lower left* PCA ordination for patients only. Convex hulls, as superimposed to the ordination on axes 1 and 2, indicate the two groups of patients, *PP* and *PNP*. The gene expression pattern is much less varying for *PP* than for *PNP*, as indicated by the much smaller area of the polygon around the *PP* group. Therefore, the osteoporotic phenotype is characterized by downregulated expression of genes included. It is also seen that no *PNP* is found within the area of the *PP* polygon, showing that none of the *PNP*s' expression pattern overlaps that of the *PP*s (i.e., the expression patterns for osteoporotic patients and non-osteoporotics are unambiguously separated). *Right* Canonical Variates Analysis (CVA, or discriminant analysis) of gene expression patterns in bone tissues of osteoporotic patients (*PP, white bars*), and non-osteoporotic individuals (*PNP, black bars*). CVA provides canonical axes in order to maximize separation of a priori defined groups of observations (here, the 7 *PP* and 10 *PNP*). Since the number of axes that can be derived is one less than the number of groups (here two groups), in our case CVA did not allow display by two-dimensional scatter diagrams, and separation of osteoporotic and non-osteoporotic patients is expressed by the scores for observations (i.e., patients) along this single canonical axis. Note the strong discriminatory power of the scores for gene expression patterns for the human orthologs of the deer genes as shown by the perfect segregation of the *PP* and *PNP* groups, i.e., the scores for the gene expression patterns of the osteoporotic patients and the non-osteoporotic individuals separate widely (i.e., the gap separating the groups extends between +4 and −6)

were detected in the cells of the antler cartilage (Fig. 3, ESM Fig. S3), (c) we calculated 2- to 7-fold overexpressions in the antler cartilage versus the fetal growth plate cartilage for matrix genes like *col1A1*, *col1A2*, *sparc* as well as their "upregulators" *osx* and *runx2* (ESM Table S1).

Antler: on the robust bone development

In contrast to the cartilage we find more complexity (and more gaps) when attempting to envisage a path toward the local upregulation of *runx2* in the antler bone. One possible scenario is that a diffusible morphogen leaves the sensory nerves, which innervate the velvet dermis and the periosteum (as demonstrated by Gray et al. 1992) and these molecules trigger and establish the enhanced synthesis of receptors and/or ligands in osteoblasts (e.g., the PTH/PTHrP, TGFB/BMP, ECM, and FGF2 containing complexes, which are all positive regulators of *runx2* expression). The best candidate for a such diffusible neuropeptide, acting as a local morphogen for the antler bone, is the CGRP, which is known to be abundant in the sensory nerve terminals, including those which infiltrate bone. The anabolic role of CGRP in bone metabolism has been demonstrated by its enhancing effect on Osteocalcin and PTH expressivity, both involved in bone matrix formation (Vignery and Mcarthy 1996; Hock et al. 1988). The regulatory role of CGRP in *runx2* expression has been reported recently in osteoblasts (Yang et al. 2009). The (very rich) sensory innervation of the antler comes from the *nervus trigeminus*, where the putative antler growth center (AGC) is located (Bubenik 1990). This anatomical separation could explain why a CGRP initiated morphogenic activity should be localized in the antler, including its bony part. Downstream the initiating step, in a later stage the osteoblasts can maintain those gene expressions which finally would stimulate

the *runx2* self enhancements. The synthesis of various BMP-s, FGF and TGFB-s has convincingly been demonstrated in the antler before (Mundy et al. 2001; Feng et al. 1995, 1997; Francis and Suttie 1998). The upregulated *runx2* activates its downstream targets, the mineralization and matrix genes, as well as the *osteocalcin* gene. The expected final results of the above events are the very high-energy consumption (due to the very intensive protein synthesis) and the exhaustive depletion of the minerals from the bloodstream by either Col1A1 or by the other mineral binding matrix proteins. To maintain the homeostasis of the calcium level in the circulation, the extracted calcium and the other minerals are supplemented from the dietary intake (which is insufficient to support antler growth) and from the skeletal bone resorption (as proposed by Banks et al. 1968a, b, and modeled by Moen et al. 1999; Moen and Pastor 1996).

Our observations and experimental data support the above notion at several points. (a) The conical shape of the calcification density at the upper regions of the already ossified antler, as shown in the sagittal cross-section of the antler (Fig. 1, Banks and Newbray 1981a, b), may be the "footprint" of a gradient of a morphogen factor (e.g., CGRP), which diffuses inward from the velvet dermis. (b) The expression of *runx2*, *osx* and their downstream regulated mineralization genes was much higher in the antler bone than in the skeletal samples. (c) Our GC–MS experiments were consistent with the high-energy requirement of the high-expression genes in the antler bone, as was shown by the high glucose content of the antler bone versus the vertebrae (nearly fivefold). (d) This high glucose consumption was in accordance with the high expression of the gene *osteocalcin* (*oc*). The activity of *oc* was known to ensure the elevated insulin synthesis and sensitivity required for glucose utilization (Lee et al. 2007) (compare Figs. 1d, 2; Table 5). Further quantitative GC–MS measurements provided additional supporting data for our suggestion. (e) The hydroxyproline contents indicated much less collagen decay in the antler bone than in the vertebra, which was in harmony with the intensive *col1A1* expression in the antler. (f) The much lower ethanolamine-phosphate and the reduced free phosphate content in the antler bone versus the vertebra and rib bones were concordant with the unidirectional ("antlerward") flow of minerals from the skeleton and deposition of the minerals in the antler bone matrix.

Considering our results and the previous findings, we suggest that the high (10- to 30-fold or more) activity of the mineralization genes and the resulting high mass of the antler organic matrix is sufficient to govern the flow toward the antler and there is no need for the active inhibition of mineral deposition in the skeletal bones.

Genes and regulatory mechanisms, which are revealed in this article support vigorous and rapid bone tissue deposition. We believe that studying the robust bone development of deer could facilitate and revive biomedical research on the field of osteoporosis treatment and bone replacement therapies. An example was shown here by using the gene expression data of this article: when we compared the expression pattern of the human orthologous genes of the deer genes upregulated in the antler bone, in osteoporotic and non-osteoporotic groups of patients, a very unambiguous segregation (of the groups) was achieved (Fig. 5).

Acknowledgments The authors are indebted to Magdolna Tóth Péli, Csilla Sánta Török, Kornélia Szóráth Gálné for excellent technical assistance, to MSc students András Berta and Attila Hegedűs (ELTE, Budapest) for enthusiastic help. Thanks are due to Péter Orosz and Natalia Polgár for critical reading of the manuscript, and to Sankar Adhya (NIH, Bethesda), László Sugár (U. Kaposvár), Ernő Duda (BRC, Szeged) and János Szabad (U. Szeged), Sándor Spisák, Bernadett Balla and János Kósa (SOTE, Budapest) for their constant interest. This work was supported by grants OTKA T032205 to L.O., OM 0320/2004 to L.O., NKFP 1A/007/2004 to L.O. and P.L., 454/2003 and 006/2009 from the Ministry of Health, Social and Family Affairs, ETT-ESKI to L.O., OTKA PD75496 to S.S., and by the János Bolyai fellowship of the HAS to S.S.

References

Alvarez L, Oriola J, Jo J, Ferró T, Pons F, Peris P, Guañabens N, Durán M, Monegal A, Martínez de Osaba MJ, Rivera-Fillat F, Ballesta AM (1999) Collagen type I alpha1 gene Sp1 polymorphism in premenopausal women with primary osteoporosis: improved detection of Sp1 binding site polymorphism in the collagen type 1 gene. Clin Chem 45(6 Pt 1):904–906

Balla B, Kósa JP, Kiss J, Borsy A, Podani J, Takács I, Lazáry Á, Nagy Zs, Bácsi K, Speer G, Orosz L, Lakatos P (2007) Different gene expression patterns in the bone tissue of aging postmenopausal osteoporotic women. Calcif Tissue Int 82(1):12–26

Banks WJ, Newbray JW (1981a) Antler development as a unique modification of mammalian endochondral ossification, Fig. 6. Antler development of Cervidae (part II, Ed. Brown RD) Texas A I University Kingsvile, Texas 78363:285

Banks WJ, Newbrey JW (1981b) Antler development as a unique modification of mammalian endochondral ossification, Fig. 12. Antler development of Cervidae (part II, Ed. Brown RD) Texas A I University Kingsvile, Texas 78363:285

Banks WJ, Newbrey JW (1983) Light microscopic studies of the ossification process in developing antlers. In: Brown RD (ed) Antler development in Cervidae. Caesar Kleburg Wildlife Research Institute, Kingsville, pp 231–260

Banks W, Epling J, Kainer R, Davis R (1968a) Antler growth and osteoporosis, I. Morphological and morphometric changes in the costal compacta during the antler growth cycle. Anat Rec 162:387–398

Banks W, Epling J, Kainer R, Davis R (1968b) Antler growth and osteoporosis, II. Gravimetric and chemical changes in the antler growth cycle. Anat Rec 162:399–406

Barta E, Sebestyén E, Pálfy TB, Tóth G, Ortutay CP, Patthy L (2005) DoOP: Databases of Orthologous Promoters, collections of clusters of orthologous upstream sequences from chordates and plants. Nucleic Acids Res 33(Database issue): D86–D90

Borsy A, Podani J, Stéger V, Balla B, Horváth A, Kósa JP, Gyurján I Jr, Molnár A, Szabolcsi Z, Szabó L, Jakó E, Zomborszky Z, Nagy J, Semsey S, Vellai T, Lakatos P, Orosz L (2009) Identifying novel genes involved in both deer physiological and human pathological osteoporosis. Mol Genet Genomics 281:301–313

Bubenik GA (1990) The role of the nervous system in the growth of antlers. In: Bubenik GA, Bubenik AB (eds) Horns, pronghorns and antlers. Springer, Hamburg, pp 339–358

Chapman D, Larkmead, Mills B, Bury S (1975) Antler-bone of contention. Mammal Rev 5:No. 4

Faucheux C, Price JS (1999): Parathyroid hormone-related peptide may play a role in deer antler regeneration. In: Danks J, Dacke C Flik G, Gay C (ed): Calcium metabolism: comparative endocrinology. BioScientifica Ltd, Bristol. pp 131–138

Faucheux C, Horton MA, Price JS (2002) Nuclear localization of type I parathyroid hormone/parathyroid hormone-related protein receptors in deer antler osteoclasts: evidence for parathyroid hormone-related protein and receptor activator of NF-kappaB-dependent effects on osteoclast formation in regenerating mammalian bone. J Bone Miner Res 17:455–464

Feng JQ, Chen D, Esparza J, Harris MA, Mundy GR, Harris SE (1995) Deer antler tissue contains two types of bone morphogenetic protein 4 mRNA transcripts. Biochim Biophys Acta 1263:163–168

Feng JQ, Chen D, Ghosh-Choudhury N, Esparza J, Mundy GR, Harris SE (1997) Bone morphogenetic protein 2 transcripts in rapidly developing deer antler tissue contain an extended 5′ non-coding region arising from a distal promoter. Biochim Biophys Acta 1350:47–52

Francis SM, Suttie JM (1998) Detection of growth factors and proto-oncogene mRNA in the growing tip of red deer (*Cervus elaphus*) antler using reverse-transcriptase polymerase chain reaction (RT-PCR). J Exp Zool 281:36–42

Galamb O, Spisák S, Sipos F, Tóth K, Solymosi N, Wichmann B, Krenács T, Valcz G, Tulassay Z, Molnár B (2010) Reversal of gene expression changes in the colorectal normal-adenoma pathway by NS398 selective COX2 inhibitor. Br J Cancer 102(4):765–773

Gray C, Hukkanen M, Konttinen YT, Terenghi G, Arnett TR et al (1992) Rapid neural growth: calcitonin gene-related peptide and substance P-containing nerves attain exceptional growth rates in regenerating deer antler. Neuroscience 50:953–963

Gyurján J-I, Molnár A, Borsy A, Stéger V, Hackler J-L, Zomborszky Z, Papp P, Duda E, Deák F, Lakatos P, Puskás LG, Orosz L (2007) Gene expression dynamics in deer antler: mesenchymal differentiation toward chondrogenesis. Mol Genet Genomics 277:221–235

Hock J, Centrella M, Canalis E (1988) Insulin-like growth factor I has independent effects on bone matrix formation and cell replication. Endocrinology 122:254–260

Jin H, van't Hof R, Albagha O, Ralston S (2009) Promoter and intron 1 polymorphisms of COL1A1 interact to regulate transcription and susceptibility to osteoporosis. Hum Mol Genet 18(15):2729–2738

Kohen MM Jr (2009) Perspectives on RUNX genes: an update. Am J Med Genet A 149A(12):2629–2646

Komori T (2010) Regulation of bone development, extracellular matrix protein genes by RUNX2. Cell Tissue Res 9(1):189–195

Korpos É, Molnár A, Papp P, Kiss I, Orosz L, Deák F (2005) Expression pattern of matrilins and other extracellular matrix proteins characterize distinct stages of cell differentiation during antler development. Matrix Biol 24:124–135

Lee NK, Sowa H, Hinoi E, Ferron M, Ahn JD, Confavreux C, Dacquin R, Mee PJ, McKee MD, Jung DY, Zhang Z, Kim JK, Mauvais-Jarvis F, Ducy P, Karsenty G (2007) Endocrine regulation of energy metabolism by the skeleton. Cell 130(3):456–469

Li C, Suttie JM (2001) Deer antlerogenic periosteum: a piece of postnatally retained embryonic tissue? Anat Embryol 204:375–388

Li C, Clark DE, Lord EA, Stanton J, Suttie JM (2002) Sampling technique to discriminate the different tissue layers of growing antler tips for gene discovery. Anat Rec 268:125–130

Moen R, Pastor J (1996) Simulating antler growth and energy, nitrogen, calcium and phosphorus metabolism in caribou. Rangifer, Special Issue 10:85–98

Moen R, Pastor J, Cohen Y (1999) Antler growth and extinction of Irish elk. Evol Ecol Res 1:235–249

Molnar A, Gyurjan I, Korpos E, Borsy A, Steger V, Buzas Z, Kiss I, Zomborszky Z, Papp P, Deak F, Orosz L (2007) Identification of differentially expressed genes in the developing antler of red deer *Cervus elaphus*. Mol Genet Genomics 277:237–248

Mundy G, Gutierrez G, Gallwitz W et al (2001) Antler-derived bone growth factors and their potential for use in osteoporosis. In: Sim JS, Sunwoo HH, Hudson RJ, Jeon BT (eds) Antler science and product technology. Antler Science and Production Technology Research Centre, Canada, pp 171–187

Nakashima K, Zhou X, Kunkel G, Zhang Z, Min D, Behringer R, Crombrugghe B (2002) The novel zinc finger-containing transcription factor osterix is required for osteoblast differentiation and bone formation. Cell 108:17–29

Nikiforova V, Kopka J, Tolstikov V, Fiehn O, Hopkins L, Hawkesford M, Hesse H, Hoefgen R (2005) Systems rebalancing of metabolism in response to sulfur deprivation, as revealed by metabolome analysis of Arabidopsis plants. Plant Physiol 138(1):304–318

Podani J (2001) SYN-TAX 2000 user's manual. Scientia Publishing, Budapest

Price J, Allen S (2004) Exploring the mechanisms regulating regeneration of deer antlers. Philos Trans R Soc Lond 359:809–822

Price J, Oyajobi O, Nalin M, Frazer A, Russell G, Sandell J (1996) Chondrogenesis in the regenerating antler tip in red deer: expression of collagen types I, IIA, IIB, and X demonstrated by in situ nucleic acid hybridization and immunocytochemistry. Dev Dyn 205:332–347

Price J, Allen S, Faucheux C, Althanaian T, Mount J (2005) Deer antlers: a zoological curiosity or the key to understanding organ regeneration in mammals? J Anat 207:603–618

Puskás L, Hackler L Jr, Kovács G, Kupihár Z, Zvara A, Micsik T, van Hummelen P (2002) Recovery of cyanine-dye nucleotide triphosphates. Anal Biochem 305(2):279–281

Rucklidge GJ, Milne G, Bos KJ, Farquharson C, Robins SP (1997) Deer antler does not represent a typical endochondral growth system: immunoidentification of collagen type X but little collagen type II in growing antler tissue. Comp Biochem Physiol B Biochem Mol Biol 118:303–308

Sambrook J, Fritsch EF, Maniatis T (1989) Methods of screening. In: Nolan C (ed) Molecular cloning, a laboratory manual. Cold Spring Harbor Laboratory Press, New York

Siebel M, Eastell R, Gundberg C, Hannon R, Pols H (2002) Biochemical markers of bone metabolism in bk. In: Bilezikian J, Raisz L, Rodan G (eds) Principles of bone biology, Academic press, New York, pp 1543–1549

Stein G, Lian J, Montecino M, Wijnen A, Stein J, Javed A, Zaidi K (2002) Involvement of nuclear architecture in regulating gene expression in bone cells in bk. In: Bilezikian J, Raisz L, Rodan G (eds) Principles of bone biology, Academic press, New York, pp 177–178

Vignery A, Mcarthy TL (1996) The neuropeptide calcitonin gene-related peptide stimulates insulin-like growth factor I production by primary fetal rat osteoblasts. Bone 18:331

Villányi Z, Gyurján I, Stéger V, Orosz L (2008) Plaque based competitive hybridization. J Biomol Screen 13:80–84

Whyte M (2002) Hypophosphatasia in bk. In: Bilezikian J, Raisz L, Rodan G (eds) Principles of bone biology. Academic press, New York, pp 1235–1236

Yang C, Wang Z, Zhao H, Yao Y, Chen P (2009) The regulatory effect of calcitonin gene-related peptide on bone metabolism of osteoblast cells co-cultured with breast cancer cells. Tumor 29(9):833–837